Soft Matter

Swelling Responses of Surface-Attached Bottlebrush Polymer Networks

Journal:	*Soft Matter*
Manuscript ID	SM-ART-05-2018-001127.R1
Article Type:	Paper
Date Submitted by the Author:	20-Jul-2018
Complete List of Authors:	Mah, Adeline; University of Houston Mei, Hao; Rice University, Chemical and Biomolecular Engineering Basu, Prithvi; University of Houston Laws, Travis; University of Tennessee Ruchhoeft, Paul; University of Houston, Department of Electrical and Computer Engineering Verduzco, Rafael; Rice University, Chemical and Biomolecular Engineering Stein, Gila; University of Tennessee,

Soft Matter

FULL PAPER SUBMISSION

Where physics meets chemistry meets biology for fundamental soft matter research

2016 Impact factor: **3.889**

www.rsc.org/softmatter

Soft Matter has a global circulation and interdisciplinary audience with a particular focus on the interface between physics, biology, chemical engineering, materials science and chemistry.

The following paper has been submitted to *Soft Matter* for consideration as a **full paper**.

Soft Matter aims to publish **high quality** papers reporting on the generic science underpinning the properties, applications, and phenomena of soft matter. The primary criterion for acceptance of a contribution for publication is that it must report high-quality new science and make a significant contribution to its field. *Soft Matter* is an **interdisciplinary** journal and suitable papers should cross disciplines or be highly significant within the field from which they originate.

Routine or incremental work, however competently researched and reported, should not be recommended for publication if it does not meet our expectations with regard to novelty and impact.

Thank you for your effort in reviewing this submission. It is only through the continued service of referees that we can maintain both the high quality of the publication and the rapid response times to authors.

We would greatly appreciate if you could review this paper in **ten days**. Please let us know if that will not be possible. Please support all comments with scientific justifications or we may be unable to use your report/ask for extra feedback.

Once again, we appreciate your time in serving as a reviewer. To acknowledge this, the RSC offers a **25% discount** on its books: http://www.rsc.org/Shop/books/discounts.asp. Please also consider submitting your next manuscript to *Soft Matter*.

Best wishes,

Darrin Pochan
Editor-in-Chief, *Soft Matter*

Swelling Responses of Surface-Attached Bottlebrush Polymer Networks

Adeline Huizhen Mah,[†‡] Hao Mei,[§] Prithvi Basu,[‖] Travis S. Laws,[#] Paul Ruchhoeft,[‖] Rafael Verduzco,[§]* Gila E. Stein[#]*

[†] Materials Science and Engineering Program, University of Houston, Houston TX 77204; [‡]Department of Chemical and Biomolecular Engineering, University of Houston, Houston TX 77204; [§] Department of Chemical and Biomolecular Engineering, Rice University, Houston TX 77006; # Department of Chemical and Biomolecular Engineering, University of Tennessee, Knoxville TN 37996; [‖]Department of Electrical and Computer Engineering, University of Houston, Houston TX.

ABSTRACT

The swelling responses of thin polymer networks were examined as a function of primary polymer architecture. Thin films of linear or bottlebrush polystyrene were cast on polystyrene-grafted substrates, and surface-attached networks were prepared with a radiation crosslinking reaction. The dry and equilibrated swollen thicknesses were both determined with spectroscopic ellipsometry. The dry thickness, which reflects the insoluble fraction of the film after crosslinking, depends on the primary polymer size and radiation dose but is largely independent of primary polymer architecture. When networks are synthesized with a high radiation dose, producing a high density of crosslinks, the extent of swelling is similar for all primary polymer architectures and molecular weights. However, when networks are synthesized with a low radiation dose, the extent of swelling is reduced as the primary polymer becomes larger or increasingly

branched. These trends are consistent with a simple Flory model for equilibrium swelling that describes the effects of branch junctions and radiation crosslinks on network elasticity.

INTRODUCTION

Polymer networks can be synthesized by linking primary polymers into a larger system. Their unique sorption, responsive and mechanical properties are frequently leveraged for biomedical applications,[1] sensing,[2,3] actuation,[3] and flexible substrates.[4,5] Hydrogels are a common example of polymer networks, and are synthesized by crosslinking (or end-linking) a system of hydrated polymers. Hydrogels can hold large amounts of water, and their open structure in a swollen state can be used to immobilize enzymes and encapsulate cells.[1] Furthermore, by selecting a primary polymer that responds to an external stimulus, one can engineer a hydrogel that reversibly changes its volume for sensing and actuation.[2,3] Another known example of polymer networks is elastomers, which can be formed by crosslinking of rubbery primary polymers. The mechanical properties of elastomers are tunable through crosslink density, which makes them useful as flexible substrates for soft lithography[6] and stretchable electronics,[5] among other applications.

The swelling thermodynamics of polymer networks is a well-studied problem, as measurements of equilibrium swelling are used to quantify effective crosslink density, average length of network chains, and junction functionality in all types of polymer networks.[7] The models of Flory and Rehner,[8–10] which calculate the free

energy of swelling by assuming that mixing processes and elastic deformations are separable, can successfully describe the behaviors of many crosslinked systems. Many studies have used these models to characterize the structure of bulk networks based on linear primary polymers. However, polymer architecture is an important variable in materials design, as it controls surface/interface interactions, processability, and mechanics.[11] Networks prepared from branched primary polymers, such as stars and combs, can exhibit different swelling responses than their linear analogues.[12–14] For example, swelling of star polymer networks can decline as arm length is reduced, because arm length sets an upper limit on the molecular weight between crosslinks.[13,14] Furthermore, in networks based on comb primary architectures, the kinetics of swelling and deswelling are enhanced by the mobile side-chains.[15,16] Therefore, to leverage the unique properties of branched polymers in networks, it is important to characterize both the network topology and swelling responses.

The objective of this work is to examine the structure and swelling responses of bottlebrush polystyrene networks. Bottlebrushes are a highly branched structure with one side chain (i.e., branch) per backbone monomer.[17,18] Steric repulsion between side chains will induce backbone extension, leading to rod-like or worm-like conformations. These unusual conformations will prevent chain entanglements, producing an unusually soft and processable material.[19–21] Furthermore, the brush-like structure can introduce new surface and interface functions,[22] much like those encountered in surface-attached polymer brushes.[23] Polystyrenes are not viable as elastomers or hydrogels, but this chemistry is very useful for fundamental studies of polymer networks: both linear and bottlebrush

architectures are easy to synthesize, and the interactions between polystyrene and different organic solvents are well characterized.

We prepared thin, surface-attached networks using a one-step radiation crosslinking reaction. Thin film confinement will restrict the swelling to one-dimension, which produces a large and rapid response (thickness change) that is easily detected with ellipsometry.[24] The swelling behaviors of the bottlebrush-based networks are compared with networks derived from linear analogues, and experimental data are interpreted using a form of the Flory-Rehner model that accounts for both pre-formed junctions (*i.e.*, the bottlebrush backbone) and radiation crosslinks.[8,14] We find that swelling is reduced by increasing the number of branches in the primary polymer, which is attributed to two effects: 1) shorter elastic strands, M_x, connecting network junctions; and 2) a greater concentration of elastic chains, c_e, within the network. Finally, we show that the swelling ratio of all networks with moderate to high crosslink densities will scale as $c_e^{-0.3}$, which is consistent with the theoretical prediction of $c_e^{-1/3}$.

MATERIALS AND METHODS

Materials. Unless specified, all reagents and solvents were purchased from commercially available sources and used as received. Styrene was passed through an aluminum oxide column to remove inhibitors. 2,2'-Azobis(2-methylpropionitrile) (AIBN) was purified by recrystallizing in methanol. Bicyclo[2.2.1]hept-5-en-2-ylmethyl 2-(((dodecylsulfanyl)(thioxo)methyl)sulfanyl)-2-methylpropanoate (NB-CTA)[25] and the modified 2nd generation Grubbs ((H2IMes)(-pyr)2(Cl)2RuCHPh) catalyst[26] were synthesized according to published methods.

Linear Polystyrene (PS) Homopolymers. PS standards were purchased from Scientific Polymers, Inc. Specifications are summarized in Table 1.

Table 1: Specifications of PS standards. M_w is weight-average molecular weight and $Đ$ is dispersity.

Polymer	M_w, kg/mol	$Đ$
L_60	61.8	1.07
L_214	213.6	1.01

Norbornene Functionalized Polystyrene (PS) (NB-PS-CTA) Macromonomer. Linear polystyrene macromonomers were prepared using reversible addition-fragmentation (RAFT) polymerization. NB-CTA, AIBN and toluene were added into a 10mL round bottom flask. The mol ratios of reagents are reported in Table 2. The solution was purged with nitrogen for 30 minutes and the polymerization was initiated by placing the flask in an oil bath at 70°C. After 17 hours, the flask was removed and quenched by immersing in an ice bath. The polymer was then obtained by precipitating in methanol at 4°C and dried under vacuum. NMR for a representative NB-PS-CTA macromonomer is reported in Figure S1a. SEC data for all NB-PS-CTA macromonomers are reported as dotted black lines in Figure S2.

Table 2: Mol ratios of reagents added for synthesis of PS macromonomers.

Target M_w (kg/mol)	NB-CTA: S	NB-CTA: AIBN	Toluene:S
3	1:80	10:1	1:1
8.2	1:300	10:1	1:1

Bottlebrush Polystyrene (P(NB-PS-CTA)). Bottlebrush polymers with polystyrene side chains were synthesized through ring-opening metathesis polymerization (ROMP) method using the modified 2nd generation Grubbs ((H2IMes) (-pyr)$_2$(Cl)$_2$RuCHPh) catalyst (Scheme 1). All ROMP reactions were performed in a glove box. In a 20 mL vial, a stock solution of the modified 2nd generation Grubbs catalyst was prepared with anhydrous DCM (3.49mg, 0.0048mmol, 0.95mL). Second, NB-PS-CTA (79.13mg, 0.0252mmol) was added into another 20 mL vial containing a stir bar, and anhydrous DCM was added to generate a final solution concentration of 0.05 M (0.5 mL). Next, 0.1 mL (0.0003 mmol) of the catalyst solution was added into the prepared macromonomer solution to initiate the reaction and stirred at room temperature for at least 1 hr. The reaction was quenched with 0.1 mL of butyl vinyl ether and the product was recovered through precipitation in methanol at 4°C and dried under vacuum at room temperature. This procedure is a generalized description of the ROMP reaction. Based on the GPC results, all bottlebrush PS-CTA synthesized were found to have a macromonomer conversion of >92%.

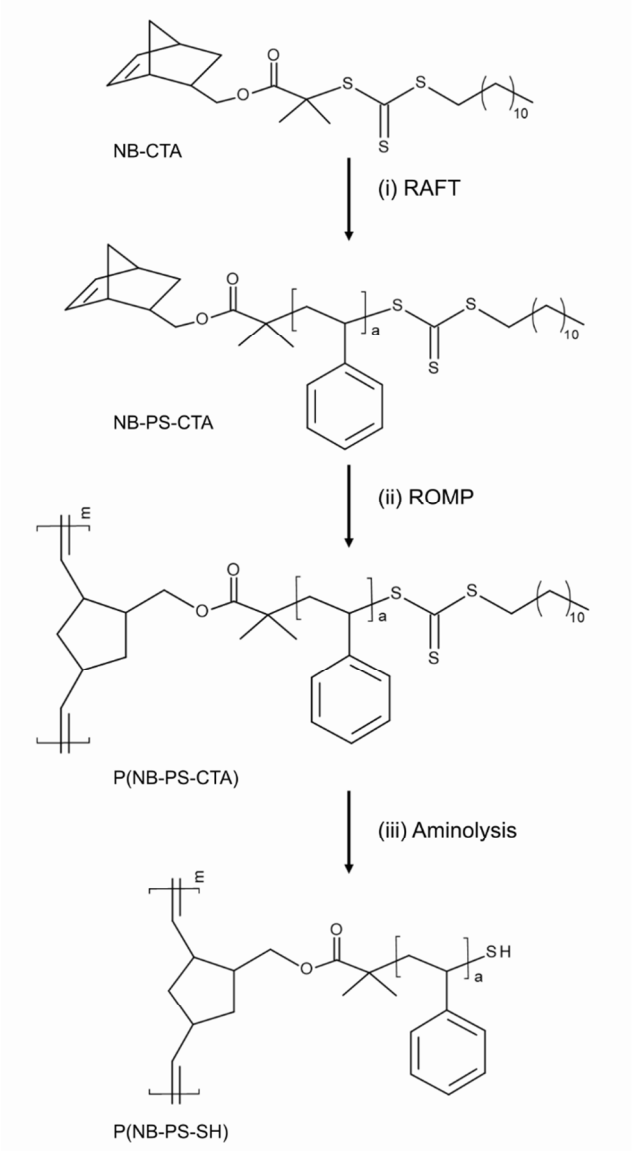

Scheme 1: Synthetic pathway of PS bottlebrush polymers. [a] Reagents and conditions: (i) AIBN, styrene, 70°C (ii) CH_2Cl_2, (H2IMes) $(pyr)_2(Cl)_2RuCHPh$ (iii) 1,4-dioxane, hexylamine, tributylphosphine.

Thiol-Terminated Bottlebrush Polystyrene (P(NB-PS-SH)). Bottlebrush PS-SH was prepared by removing the chain transfer agent (CTA) end-group via an aminolysis reaction (Scheme 1). This reaction was performed in the glove box. Bottlebrush PS-CTA was dissolved with 1,4-dioxane and stirred for 12 h at room temperature in the presence of hexylamine and tributylphosphine. The hexylamine added was at least 10 times the

amount of CTA groups present and the tributylphosphine was added to prevent the formation of disulfide bonds[27,28]. The transition of a yellow to clear, colorless solution indicates that the reaction is complete. This is confirmed through the UV/Vis spectra obtained from the GPC which showed the disappearance of an absorbance peak at 300-310nm[27] in the bottlebrush product. The product was recovered through precipitation in methanol at 4 °C and dried under vacuum at room temperature. Table 3 summarizes the properties of bottlebrush PS-SH used in this study. Where backbone weight-average molecular weight is M_w, backbone degree of polymerization is N_b, and backbone dispersity is $Đ_b$. Weight-average molecular weight of side chains is $M_{w,sc}$ and dispersity in side chains is $Đ_{sc}$. Number average molecular weight of side chains is $M_{sc.}$

Table 3: Properties of bottlebrush PS-SH additives from SEC MALLS.

Polymer	M_w (kg/mol)	N_b [a]	$Đ_b$	$Đ_{sc}$	M_{sc} (kg/mol)
BB_60	59.7	19	1.30	---	3.2[b]
BB_200	200.9	65	1.73	---	2.8[b]
BB_65	65.4	8	1.41	1.11	7.0

[a] N_b is calculated from M_w. [b] Calculated from ^{1}H NMR.

Nuclear Magnetic Resonance Spectroscopy (NMR). Using a 400 MHz Bruker multinuclear spectrometer, the hydrogen NMR (^{1}H NMR) spectra was obtained in $CDCl_3$ with tetramethylsilane as an internal standard. Samples with a concentration of 10 mg/mL were placed in 5mm o.d. tubes. Data are reported in Figure S1.

Gel Permeation Chromatography (GPC). Molecular weights and dispersities of bottlebrushes and macromonomers were obtained using an Agilent 1200 module with

three PSS SDV columns in series (100, 1000 and 10000 Å pore sizes), an Agilent variable wavelength UV/vis detector, a Wyatt Technology HELEOS II multiangle laser light scattering (MALLS) detector (λ = 658 nm), and a Wyatt Technology Optilab rEX RI detector. This system enables size exclusion chromatography (SEC) with simultaneous refractive index (SEC-RI), UV/vis (SEC-UV/vis) and MALLS detection. THF was used as the mobile phase with a flow rate of 1mL/min at 40°C. The conversion of the bottlebrush polymers was determined by comparing the peak areas of the PS bottlebrushes and unreacted PS macromonomers. The refractive index (d*n*/d*c*) of the PS bottlebrushes were calculated with the assumption of 100% mass recovery and corrected by using the actual injected mass of PS bot in the solution. This correction accounts for the unreacted PS macromonomers during the ROMP reaction. Data are reported in Figure S2.

Spectroscopic Ellipsometry. The thicknesses of the polymer films were measured using a J.A. Woollam M-2000 spectroscopic ellipsometer. The ellipsometry parameters Δ and ψ were modeled by describing the polymer's optical properties with the Cauchy dispersion relation, $n(\lambda) = A + B/\lambda^2$, where λ is the incident wavelength (nm) where *A*, *B* and film thickness are adjustable parameters for regression analysis. All thickness measurements reported in this study are an average value of 2-5 measurements.

Atom Beam Proximity Lithography. Samples were irradiated by a broad beam of helium atoms generated by a saddle-field source similar to the design reported by Hogg.[29] With a constant flow of helium feed gas, the source generates a mixed beam of ions and atoms, the latter of which are formed through charge-exchange collisions of ions with the background helium gas. The beam drifted through 1.3 m long beamline to an exposure

station, evacuated by a turbo-molecular pump backed by a rotary pump, that housed an x-y stage for moving the sample underneath a stencil. A set of deflector plates, placed at the approximate center of the beamline, swept aside the ions to form a beam of only atoms. The energy of each atom, E_a, was approximately 1.3 x 10^{-15} J for a 10kV supply setting, since the mean energy of the atom beam is ~70-85% of the power supply potential[30,31]. To estimate the atom flux, the secondary electron current, I_{se}, was measured from an aluminum electrode placed behind a grounded plate with an aperture diameter, d, using a picoammeter (Keithley Instruments, Cleveland, OH). The atom flux was calculated as

$$J_a = \frac{4I_{se}}{\pi d^2} \cdot \frac{1}{\gamma q}, \qquad (1)$$

where q is the elementary charge and γ is the secondary electron yield, previously measured to be 1.5[32]. The exposure dose is

$$D_{ABL} = J_a E_a t_e. \quad (2)$$

For this study, the irradiation doses ranged from 1.0 to 25 mJ cm^{-2} and each exposure series was accompanied by a set of calibration exposures in PMMA. The calibration sample was used to correct for any drift in the secondary electron yield and ensure that the dose was consistent. Irradiated PS films were developed in toluene for 12 minutes and were dried with nitrogen gas immediately after development. More details of the ABL system are described elsewhere[32,33].

Substrate Preparation. Substrates used for all studies were (100)-oriented p-type silicon wafers. Each substrate was rinsed in deionized water to remove dust particles from the surface and dried under a nitrogen stream. Organic contamination was removed with an

ultraviolet-ozone cleaner, and a clean oxidized surface was confirmed with measurements of water contact angle (< 5°). A hydroxyl-terminated polystyrene was grafted to the oxidized silicon surface[34]. The hydroxy terminated PS was purchased from Scientific Polymers, Inc., and has an M_w = 5.0 kg/mol and $Đ$ = 1.1. The brush was prepared and characterized following the protocol described elsewhere[35]. The measured water contact angle of the brush layer ranges from 88-90°, and the brush thickness was 4 nm

Polystyrene Thin Films. Polystyrene solutions of 3 wt % were prepared in toluene and the solution was filtered with two 0.2 μm Teflon mesh filters. The solution was spin-casted on the brushed silicon wafers at 2500-3500 rpm for 60 s. Film thicknesses were measured with a J.A. Woollam M-2000 spectroscopic ellipsometer. The ellipsometry parameters Δ and ψ were modeled by describing the polymer's optical properties with the Cauchy dispersion relation, $n(\lambda) = A + B/\lambda^2$, where λ is the incident wavelength. The optical properties of silicon and native oxide are part of a built-in database. *A*, *B*, and film thickness are adjustable parameters for regression analysis. Typical values for *A* and *B* are 1.5 and 0.01, respectively. As-cast film thicknesses were in the range of 80 to 92 nm.

Swelling Measurements. The swollen thicknesses of crosslinked linear and bottlebrush polystyrenes were determined using ellipsometry. These measurements were conducted in a home-built liquid cell with incident and exit quartz windows at a 75° angle (relative to the sample normal). The optical constants of toluene and tetrahydrofuran (THF) were determined by placing a silicon wafer with 200 nm of thermal oxide in the cell, filling with liquid, and then measuring the ellipsometry parameters Δ and Ψ. The data were modeled with the Cauchy dispersion relation over wavelengths of 350 to 1690 nm. The outcomes for toluene and THF are $n(\lambda) = 1.47 + 0.006\lambda^{-2}$ and $n(\lambda) = 1.39 +$

$0.004\lambda^{-2}$, respectively, where λ has units of μm. To monitor the equilibrium swelling of polymer networks: Films were placed in the empty liquid cell and the dry thickness was measured. The cell was then filled with the liquid, and data were acquired every 20 s until the swelling had stabilized for at least 30 min. Data were modeled by constraining the optical constants of the solvent and optimizing the Cauchy parameters and thickness for the swollen film. Additional details can be found elsewhere.[35] After removal from the solvent, the films are immediately dried in nitrogen. The de-swelled films are re-measured to confirm the dry thickness; when crosslinked with low doses, this "after swelling" value is up to 10% lower than the initial measurement, which demonstrates that some unattached polymers are extracted during the prolonged swelling. We therefore use the "after swelling" value for dry thickness in all calculations.

RESULTS AND DISCUSSION

The objective of this work is to engineer the swelling responses of surface-attached polymer networks by varying the architecture of the polymer precursors. To interrogate these behaviors, we use a simple approach based on radiation crosslinking of surface-attached polystyrene films. The polystyrene architecture is systematically varied from linear to highly branched (star-like and bottlebrush), but the overall molecular weight is approximately constant in each series of materials. The networks are swollen in a liquid solvent, and the extent of swelling is analyzed with a Flory free energy model that accounts for the primary polymer architecture.

The experimental procedures include a detailed description of sample preparation and measurement protocols. The key points are as follows: A polystyrene brush is grafted

to a silicon substrate, and then polystyrene films are spin-casted on top of the brush. Each film/brush sample is exposed to atom beam radiation, which creates radicals through ionization (hydrogen abstraction) at the tertiary carbon of polystyrene.[36] Some of these radicals will combine and generate intermolecular crosslinks throughout the film thickness and at the film/brush interface. The result of this process is a surface-attached polystyrene network,[35] where the crosslink density and network topology are controlled by the radiation dose. After radiation crosslinking, the films are soaked in toluene or THF to remove the free polymers. The networks are then re-immersed in toluene or THF, and the swollen thicknesses are measured as a function of time with spectroscopic ellipsometry. The films swell to at least 90% of their equilibrium swollen thicknesses within 1 min, and there is no noticeable difference in the response times for linear and bottlebrush architectures. The swelling process stabilizes after 120 min for exposure doses of 1.8-3.1mJ/cm^2, and after 60 min for exposure doses of 3.7-11.1mJ/cm^2. The equilibrium thickness of the swollen polymer film is calculated by modeling the ellipsometry data. The surface-attached films do not delaminate during the prolonged swelling measurement, and the initial film thickness is recovered after the samples are removed from solvent and deswelled. Optical microscopy images for these films before and after swelling measurements are reported in Figures S3 and S4. The following plots report data for soaking and swelling in toluene, and Figures S5 to S8 include a comparison with THF. We note that the extent of swelling in THF is different from the response in toluene, which reflects the distinct polymer-solvent interactions in each system, but the parameters extracted from analysis of both data sets are highly consistent.

As a first step towards characterizing the crosslinked films, we measure the normalized residual thickness as a function of radiation dose. Normalized residual thickness is defined as

$$NRT = \frac{h + (h_{ref} - h_0)}{h_0 + (h_{ref} - h_0)} \quad (3)$$

where h is the film thickness after removing the unattached material, h_0 is the initial film thickness (before crosslinking and soaking), and $h_{ref} = 100$ nm is a reference thickness that accounts for sample-to-sample variations in h_0.[35] When $NRT \rightarrow 1$, the irradiated film resists dissolution in the good solvent, which means it is attached to the surface through a network of crosslinks. Therefore, a plot of *NRT* versus dose will highlight differences in dissolution behavior that are attributable to the underlying network topologies.

Figure 1a reports the outcomes for three primary polystyrenes with overall molecular weights of $M_w \approx 60$ kg/mol: a linear architecture, a bottlebrush with $f_2 = 8$ branches, and a bottlebrush with $f_2 = 19$ branches. Figure 1b reports the outcomes for two polystyrenes with overall molecular weights of $M_w \approx 200$ kg/mol: a linear architecture and a bottlebrush with $f_2 = 65$ branches. At a fixed radiation dose, the amount of film dissolved is largely determined by the overall size of the polymer: All three architectures with molecular weights near 60 kg/mol are collapsed onto a single curve, and a high dose is required to make those films fully insoluble in toluene. The two architectures with an overall molecular weight near ~200 kg/mol are insoluble at much lower doses than the ~ 60 kg/mol series, which is expected due to their larger size. However, the networks based on ~200 kg/mol linear primary polymers are less soluble than the bottlebrush-based analogue at low to moderate doses. This discrepancy is

attributable to the effects of entanglements: the entanglement molecular weight of linear polystyrene is in the range of $M_e \approx 13$ to 19 kg/mol,[37–39] which means a ~200 kg/mol linear architecture has approximately 12 entanglements per chain, and the dissolution behavior is presumably controlled by a combination of radiation crosslinks and trapped entanglements. Bottlebrush polymers do not entangle,[19,20] so their solubility is solely controlled by the crosslinking process.

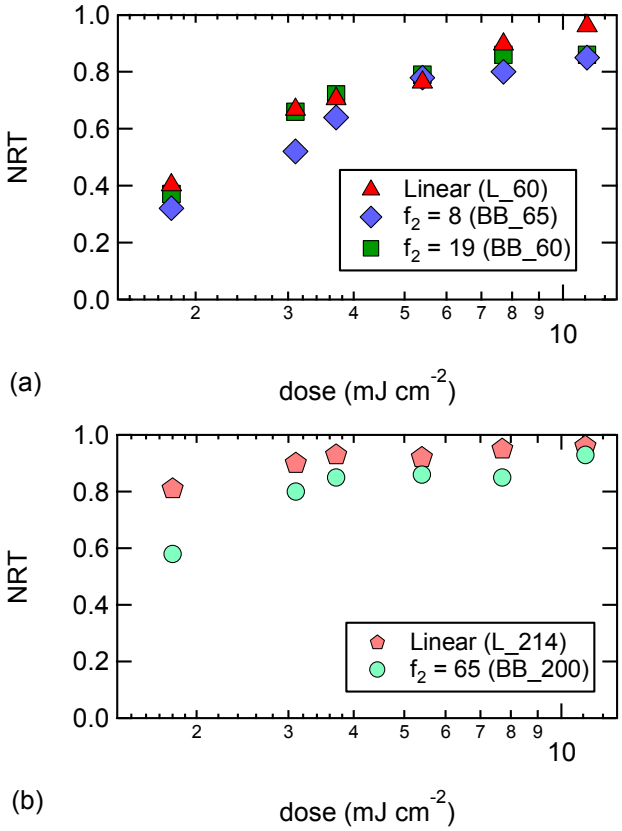

Figure 1. Normalized residual thickness (NRT) of surface-attached polystyrene networks as a function of radiation dose. Overall molecular weights of a) $M_w \approx 60$ kg/mol; and b) $M_w \approx 200$ kg/mol.

We next examine the swelling behaviors as a function of polymer architecture. Figures 2a and 2b report the swelling ratio h_e/h as a function of radiation dose for polystyrenes with $M_w \approx 60$ kg/mol and 200 kg/mol, respectively, where the parameter

h_e is the equilibrium swollen thickness. These data demonstrate that swelling behaviors are "universal" as crosslink density is increased (high doses), approaching a limit of $h_e/h \approx 3$ to 4 at the highest doses considered. However, when the crosslink density is reduced (low dose), the swelling behavior is controlled by polymer architecture and molecular weight: For a fixed molecular weight, increased branching will reduce the extent of swelling. This effect is particularly striking in the ~60 kg/mol series, where the highly branched architecture ($f_2 = 19$) experiences half the swelling of a linear architecture. For a fixed architecture, increased molecular weight will likewise reduce the extent of swelling, as observed through two comparisons: First, in the linear architecture, polymer L_214 (~200 kg/mol) swells less than polymer L_60 (~60 kg/mol) at low doses. Second, in the branched architecture, when the side-chain length is fixed but the number of branches is increased (BB_60 versus BB_200), the larger polymer (BB_200) will swell to a lesser extent.

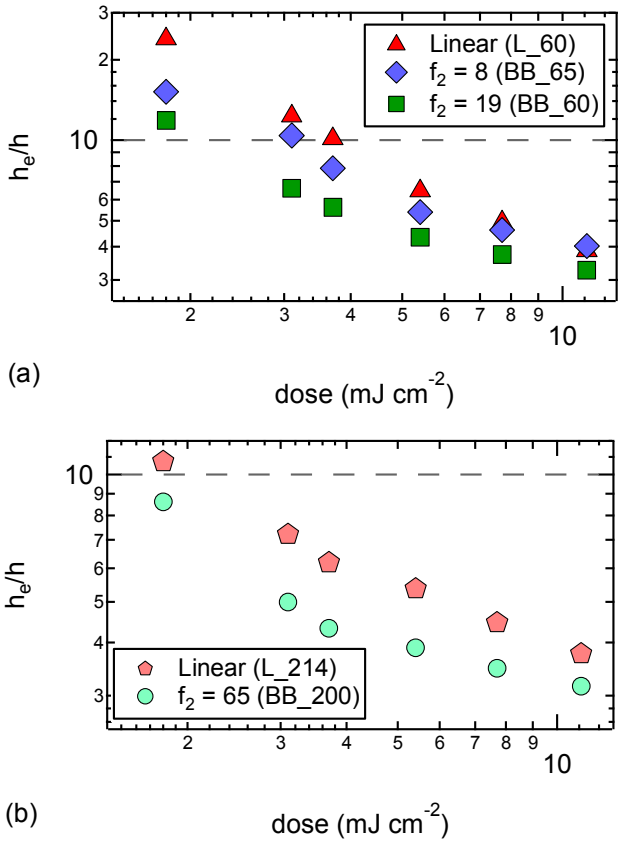

Figure 2. Swelling ratio of surface-attached polystyrene networks as a function of radiation dose. Overall molecular weights of a) $M_w \approx 60$ kg/mol; and b) $M_w \approx 200$ kg/mol. The horizontal line at h_e/h is a guide to the eye.

To better understand the architectural effects that drive these swelling behaviors, we interpret experimental data with simple models for the equilibrium swelling of surface-attached polymer films. The models are developed following the original reports by Flory[8,9] for affine deformation of Gaussian chains, and include corrections for branching,[14] surface-attachment[24] (swelling constrained to one dimension), and dangling chain ends.[8,9] The radiation crosslinks are described as tetra-functional junctions ($f_1 = 4$), while the bottlebrush backbone is treated a pre-formed junction with functionality $f_2 = N_b$. A step-by-step development of the free energy model is included in the Supporting Information. The objectives of this analysis are to determine the length of the

network chains that connect two junctions, M_x, as well as the concentration of network crosslinks that connect elastically effective chains, c_e. We note that the assumptions in these types of models can lead to inaccuracies in the calculated values of M_x and c_e, as noted in numerous literature studies.[40,41] However, these inaccuracies will not impact the trends in these data, and the trends are sufficient to understand the roles of architecture on swelling responses.

The equilibrium swelling of a surface-attached linear polymer network is described by Eq. 4:

$$\chi\phi_2^2 + \ln(1-\phi_2) + \phi_2 = \frac{\widehat{V}_1\rho}{M_x}\left[1 - \frac{2M_x}{M}\right]\left[\frac{\phi_2}{2} - \phi_2^{-1}\right] \quad (4)$$

The volume fraction of polymer in the swollen film is $\phi_2 = h_0/h_e$. The extent of swelling is controlled by the Flory interaction parameter (χ), the solvent molar volume ($\widehat{V}_1$, cm^3/mol), the polymer density ($\rho = 1.05$ g/cm^3),[37] the number-average molecular weight of the original chains (M, g/mol), and the average molecular weight between crosslinks (M_x, g/mol). The equilibrium swelling of a surface-attached bottlebrush polymer network is described by Eqn. 5, and depends on two additional parameters: the average number of side-chains on each bottlebrush (f_2), and the number-average molecular weight of the bottlebrush side chains (M_{sc}):

$$\chi\phi_2^2 + \ln(1-\phi_2) + \phi_2 = \frac{\widehat{V}_1\rho}{M_x}\left[1 - \frac{M_x}{M_{sc}}\right]\left[\left(\frac{1}{f_2\left(\frac{M_{sc}}{M_x} - 1\right)} + \frac{1}{2}\right)\phi_2 - \phi_2^{-1}\right] \quad (5)$$

As f_2 increases, the swelling behavior of a bottlebrush architecture is increasingly dominated by the tetra-functional radiation junctions. Furthermore, when the density of

crosslinks is high (M_x is low), Eqs. 4 and 5 predict the same extent of swelling in linear and branched networks, which is consistent with the trends at high dose in Figure 2.

We use Eqns. 4 and 5 to determine M_x as a function of radiation dose. All other parameters are known: ϕ_2 is measured from ellipsometry; $\widehat{V_1}$, ρ and χ are documented in the literature; and M, M_{sc}, and f_2 are measured properties of the polymers. Table 4 reports the values selected for $\widehat{V_1}$ and χ. We note that literature values of χ for each polystyrene-solvent pair are highly variable: χ for PS/THF ranges from 0.16 to 0.7,[37,42–44] and χ for PS/toluene ranges from 0.16 to 0.48 and is often dependent on polymer concentration.[37,45] Therefore, we select an average value from the literature for each system, and we do not expect measurements in different solvents to yield the exact same values of M_x. We verified that a concentration-dependent χ parameter[46] with the form$\chi = -0.27 + 0.69\phi_1$ does not change the trends in M_x as a function of dose, architecture or molecular weight.

Table 4: Solvent molar volume $\widehat{V_1}$ and Flory interaction parameter χ for PS-solvent at 25˚C.

Solvent	$\widehat{V_1}$ (cm^3/mol)	χ
Toluene	106.7	0.37[37,45]
THF	81.1	0.41[42]

The values of M_x determined by analysis of each data point (ϕ_2) with Eq. 4 or Eq. 5 are summarized in Table 5 as a function of radiation dose. These values have different implications for linear and bottlebrush architectures. Long linear polymers can entangle, so the value of M_x may reflect an effective strand length that is controlled by a

combination of trapped entanglements and radiation crosslinks. Bottlebrush polymer backbones and side-chains do not entangle, so M_x will reflect the molecular weight between radiation crosslinks along the PS side chains.

Table 5: Molecular weight between crosslinks M_x (kg/mol) for each primary polymer, from swelling in toluene (or [a]THF). L = linear, BB = bottlebrush, and the associated number designates the overall molecular weight.

Dose (mJ cm^{-2})	L_60	L_214	BB_65 ($f_2 = 8$)	BB_60 ($f_2 = 19$)	BB_200 ($f_2 = 65$)
1.8	28.9 28.8 [a]	94.0	6.96	3.22 3.21 [a]	2.79
3.1	28.4 28.6 [a]	72.4	6.91	3.16 3.05 [a]	2.69
3.7	27.8 27.4 [a]	59.6	6.81	3.12 3.09 [a]	2.62
5.4	24.5 25.4 [a]	46.9	6.42	2.98 2.88 [a]	2.54
7.7	19.9 20.9 [a]	31.1	6.09	2.82 2.89 [a]	2.43
11.1	13.8 15.1 [a]	19.6	5.64	2.61 2.69 [a]	2.29

In networks formed from linear architectures, M_x increases with the primary molecular weight. This result seems counterintuitive, as the networks formed from the larger precursor exhibit less swelling. However, the extent of swelling is controlled by the number of elastically effective chains within the network, which is less than the total number of sub-chains in the system. The principal cause of this discrepancy is "dangling" chain ends that do not contribute to network elasticity.[9] Therefore, to examine the relationship between swelling behaviors and primary polymer architecture, we use M_x to calculate the concentration of elastically effective chains, c_e. (The crosslink density is

$c_e/2$, as each chain connects two network junctions.) For the linear polystyrenes, c_e is calculated by Eq. 6,[8–10]

$$c_e = \frac{\rho}{M_x}\left[1 - \frac{2M_x}{M}\right] \quad (6)$$

For the bottlebrush polystyrenes, this concentration is calculated by Eq. 7,[9,14,47]

$$c_e = \frac{\rho}{M_x}\left[1 - \frac{M_x}{M_{sc}}\right] \quad (7)$$

The calculated values of c_e are reported in Figure 3 as a function of radiation dose for all architectures and molecular weights. When doses are high, c_e is larger for highly-branched primary polymers than linear or lightly-branched, but there is no trend with molecular weight. However, when doses are low, c_e depends on the architecture and molecular weight of the primary polymer. For the linear architecture, c_e increases with the primary molecular weight. There are two trends in the bottlebrush architectures: 1) For a fixed overall molecular weight, c_e increases with the number of side-chains. Note that as the number of side-chains increases, their lengths are decreased to maintain a constant overall molecular weight, so we could equivalently state that c_e increases as side chain length decreases. 2) For a fixed side-chain length, c_e increases with the number of side-chains/overall molecular weight. Finally, when comparing different primary architectures of the same molecular weight, c_e is higher for bottlebrush polymers compared with the linear polymer. These data suggest that radiation crosslinking will produce a larger concentration of elastically effective chains when the primary polymers are large and/or highly branched.

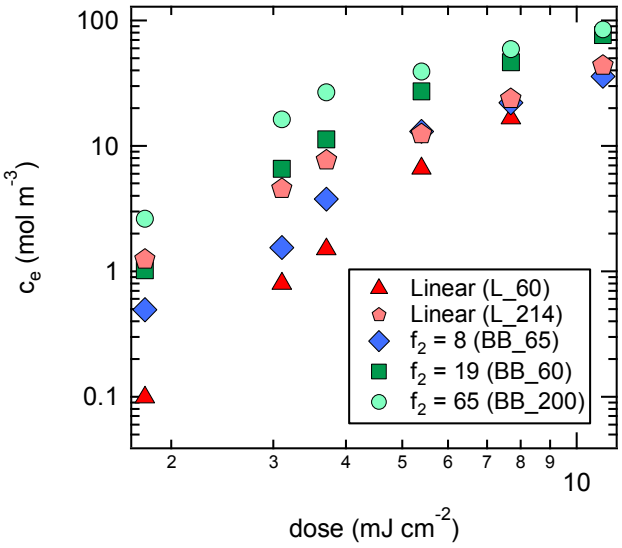

Figure 3. Calculated concentration of elastically effective chains (c_e) as a function of radiation dose.

All data are collapsed on a single master curve when the measured swelling ratio h_e/h is plotted as a function of the calculated elastic chain concentration c_e, as demonstrated in Figure 4. The scaling is approximately $h_e/h \sim c_e^{-0.3}$ for $c_e > 2$ mol/m^3, and is consistent with the expected behavior for Eq. 4 and Eq. 5 in the limit of high crosslink density (small M_x):

$$\frac{h_e}{h} \propto \left[\left(\frac{1}{2} - \chi\right)\frac{1}{\widehat{V}_1}\right]^{1/3} c_e^{-1/3} \quad (8)$$

The agreement among all data sets offers validation for the trends determined by these simple models.

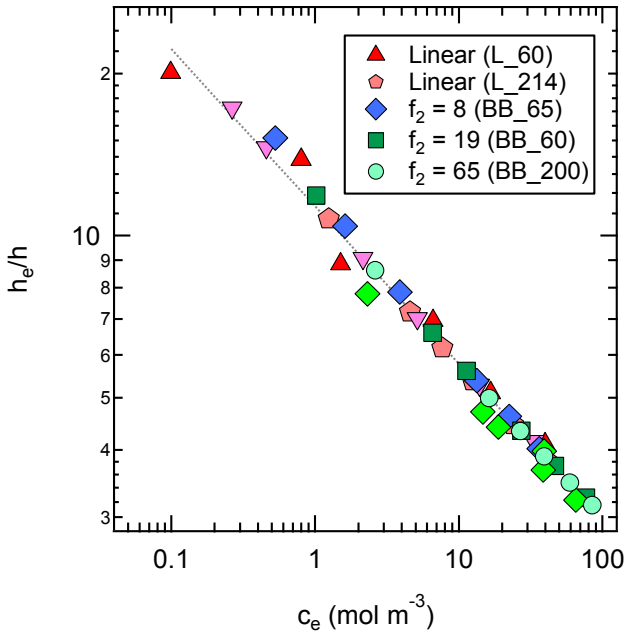

Figure 4. Measured swelling ratio (h_e/h) as a function of calculated concentration of elastically effective chains (c_e). Grey line marks the scaling $h_e/h \sim c_e^{-0.3}$.

CONCLUSIONS

We examined the swelling response of surface-attached polymer networks as a function of primary polymer architecture and molecular weight. All networks were synthesized with a radiation crosslinking reaction, and radiation dose was varied to produce a range of crosslink densities. First, we measured the normalized residual thickness (NRT) as a function of radiation dose for all networks. The residual thickness is the amount of material that is attached to the substrate through network crosslinks, so NRT is a measure of the insoluble fraction of the film. These data demonstrate that network formation depends on the overall size of the primary polymer, but it is largely independent of architecture. Second, we measured the extent of swelling as a function of radiation dose for all networks. We find that swelling declines as the primary polymer becomes increasingly branched, or as the primary polymer increases in size. This effect vanishes in the limit of high crosslink densities. Finally, we interpret the swelling data using a modified form of the Flory-Rehner theory. This analysis demonstrates that swelling is reduced with increased branching of the primary polymer because 1) the lengths of elastic chains are limited by the length of the branches; and 2) the concentration of elastic chains is increasing with the number of branches.

Surface-attached bottlebrush polymer networks could have applications in coatings, sensors and biomaterials: The brushy architecture is useful to create surfaces that resist fouling or respond to environmental cues.[23,48] The crosslinking process provides stability in harsh solvent environments, preventing delamination and other mechanical failures. The rapid swelling kinetics and tunable response (thickness change) are valuable for the detection of chemical or biological species, and the large number of end-functional side

chains can be used to bind analytes or nanoparticles.[49,50] Finally, networks synthesized by random crosslinking of bottlebrush polymers are more resistant to swelling than their linear analogues, which is valuable from a processing perspective: fewer crosslinks are needed, which lowers the dose for a radiation-activated reaction.

CONFLICTS OF INTEREST

There are no conflicts of interest to declare.

ACKNOWLEDGMENTS

A.H. Mah, T.S. Laws and G.E. Stein acknowledge financial support from the National Science Foundation under Grant No. CMMI-1740457. H. Mei and R. Verduzco acknowledge financial support from the National Science Foundation under Grant No. CMMI-1563008. P. Basu and P. Ruchhoeft acknowledge financial support from the National Science Foundation under Grant No. EEC-1530753.

REFERENCES

1 Peppas N. A., Hilt J. Z., Khademhosseini A. and Langer R., *Adv. Mater.*, 2006, **18**, 1345–1360.
2 Z. Cai, N. L. Smith, J.-T. Zhang and S. A. Asher, *Anal. Chem.*, 2015, **87**, 5013–5025.
3 White Evan M., Yatvin Jeremy, Grubbs Joe B., Bilbrey Jenna A. and Locklin Jason, *J. Polym. Sci. Part B Polym. Phys.*, 2013, **51**, 1084–1099.
4 D. Simon, T. Ware, R. Marcotte, B. R. Lund, D. W. Smith, M. Di Prima, R. L. Rennaker and W. Voit, *Biomed. Microdevices*, 2013, **15**, 925–939.
5 Y. Liu, M. Pharr and G. A. Salvatore, *ACS Nano*, 2017, **11**, 9614–9635.
6 Y. Xia and G. M. Whitesides, *Annu. Rev. Mater. Sci.*, 1998, **28**, 153–184.
7 S. Schlögl, M.-L. Trutschel, W. Chassé, G. Riess and K. Saalwächter, *Macromolecules*, 2014, **47**, 2759–2773.
8 P. J. Flory, *J. Chem. Phys.*, 1950, **18**, 108–111.
9 P. J. Flory, *Principles of Polymer Chemistry*, Cornell University Press, 1953.
10 P. J. Flory and J. Rehner, *J. Chem. Phys.*, 1943, **11**, 521–526.

11 G. Polymeropoulos, G. Zapsas, K. Ntetsikas, P. Bilalis, Y. Gnanou and N. Hadjichristidis, *Macromolecules*, 2017, **50**, 1253–1290.
12 M. Vamvakaki, S. C. Hadjiyannakou, E. Loizidou, C. S. Patrickios, S. P. Armes and N. C. Billingham, *Chem. Mater.*, 2001, **13**, 4738–4744.
13 K. B. Keys, F. M. Andreopoulos and N. A. Peppas, *Macromolecules*, 1998, **31**, 8149–8156.
14 L. G. Cima and S. T. Lopina, *Macromolecules*, 1995, **28**, 6787–6794.
15 M. Annaka, C. Tanaka, T. Nakahira, M. Sugiyama, T. Aoyagi and T. Okano, *Macromolecules*, 2002, **35**, 8173–8179.
16 Liu Qunfeng, Zhang Ping and Lu Mangeng, *J. Polym. Sci. Part Polym. Chem.*, 2005, **43**, 2615–2624.
17 S. S. Sheiko, B. S. Sumerlin and K. Matyjaszewski, *Prog. Polym. Sci.*, 2008, **33**, 759–785.
18 R. Verduzco, X. Li, S. L. Pesek and G. E. Stein, *Chem. Soc. Rev.*, 2015, **44**, 2405–2420.
19 S. J. Dalsin, M. A. Hillmyer and F. S. Bates, *ACS Macro Lett.*, 2014, **3**, 423–427.
20 W. F. M. Daniel, J. Burdyńska, M. Vatankhah-Varnoosfaderani, K. Matyjaszewski, J. Paturej, M. Rubinstein, A. V. Dobrynin and S. S. Sheiko, *Nat. Mater.*, 2016, **15**, 183–189.
21 L.-H. Cai, T. E. Kodger, R. E. Guerra, A. F. Pegoraro, M. Rubinstein and D. A. Weitz, *Adv. Mater.*, 2015, **27**, 5132–5140.
22 X. Li, S. L. Prukop, S. L. Biswal and R. Verduzco, *Macromolecules*, 2012, **45**, 7118–7127.
23 W.-L. Chen, R. Cordero, H. Tran and C. K. Ober, 50th Anniversary Perspective, https://pubs.acs.org/doi/full/10.1021/acs.macromol.7b00450, (accessed April 19, 2018).
24 R. Toomey, D. Freidank and J. Rühe, *Macromolecules*, 2004, **37**, 882–887.
25 Z. Li, K. Zhang, J. Ma, C. Cheng and K. L. Wooley, *J. Polym. Sci. Part Polym. Chem.*, 2009, **47**, 5557–5563.
26 M. S. Sanford, J. A. Love and R. H. Grubbs, *Organometallics*, 2001, **20**, 5314–5318.
27 M. Li, P. De, S. R. Gondi and B. S. Sumerlin, *J. Polym. Sci. Part Polym. Chem.*, 2008, **46**, 5093–5100.
28 A. B. Lowe, *Polym. Chem.*, 2010, **1**, 17–36.
29 A. M. Hogg, *Int. J. Mass Spectrom. Ion Phys.*, 1983, **49**, 25–34.
30 J. Franks and A. M. Ghander, *Vacuum*, 1974, **24**, 489–491.
31 M. Khorossany and R. Fitch, *Vacuum*, 1977, **27**, 159–162.
32 A. Nasrullah, *PhD Thesis*.
33 A. Nasrullah, D. Smith, T. Sherlock, P. Ruchhoeft and D. Litvinov, *J. Vac. Sci. Technol. B Microelectron. Nanometer Struct. Process. Meas. Phenom.*, 2009, **27**, 2674–2678.
34 P. Mansky, Y. Liu, E. Huang, T. P. Russell and C. Hawker, *Science*, 1997, **275**, 1458–1460.
35 Vaselabadi Saeed Ahmadi, Shakarisaz David, Ruchhoeft Paul, Strzalka Joseph and Stein Gila E., *J. Polym. Sci. Part B Polym. Phys.*, 2016, **54**, 1074–1086.
36 N. P. Cheremisinoff, *Handbook of Polymer Science and Technology*, CRC Press, 1989.

37 J. Brandrup, E. H. Immergut and E. A. Grulke, Eds., *Polymer Handbook*, Wiley-Interscience: A John Wiley & Sons, Inc., Publication, 4th edn., 1999, vol. 2.
38 L. J. Fetters, D. J. Lohse, D. Richter, T. A. Witten and A. Zirkel, *Macromolecules*, 1994, **27**, 4639–4647.
39 R. H. Rubinstein Michael, Colby, *Polymer Physics*, Oxford University Press, 2003.
40 J. L. Valentín, J. Carretero-González, I. Mora-Barrantes, W. Chassé and K. Saalwächter, *Macromolecules*, 2008, **41**, 4717–4729.
41 G. Hild, *Polymer*, 1997, **38**, 3279–3293.
42 J. A. Emerson, D. T. W. Toolan, J. R. Howse, E. M. Furst and T. H. Epps, *Macromolecules*, 2013, **46**, 6533–6540.
43 T. Shiomi, K. Kuroki, A. Kobayashi, H. Nikaido, M. Yokoyama, Y. Tezuka and K. Imai, *Polymer*, 1995, **36**, 2443–2449.
44 Narasimhan Venkataraman, Huang Robert Y. M. and Burns Charles M., *J. Polym. Sci. Polym. Phys. Ed.*, 2003, **21**, 1993–2001.
45 A. F. M. Barton, *Handbook of Polymer-Liquid Interaction Parameters and Solubility Parameters*, CRC Press, 1990.
46 C. M. Hansen, *Hansen Solubility Parameters: A User's Handbook, Second Edition*, CRC Press, 2012.
47 A. H. Mah, University of Houston, 2018.
48 M. A. C. Stuart, W. T. S. Huck, J. Genzer, M. Müller, C. Ober, M. Stamm, G. B. Sukhorukov, I. Szleifer, V. V. Tsukruk, M. Urban, F. Winnik, S. Zauscher, I. Luzinov and S. Minko, *Nat. Mater.*, 2010, **9**, 101–113.
49 C. Wang, N. T. Flynn and R. Langer, *Adv. Mater.*, 2004, **16**, 1074–1079.
50 H. R. Culver, J. R. Clegg and N. A. Peppas, *Acc. Chem. Res.*, 2017, **50**, 170–178.

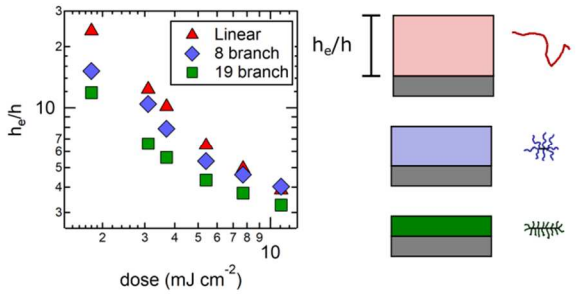

The swelling of surface-attached polymer networks (h_e/h) is reduced with increased branching of the primary polymer.